I J C T A, 9(7), 2016, pp. 3373-3389

Effect of Process Parameters on Mechanical Properties and Modeling of Pulsed TIG Welding of Inconel 718 Alloy

P. Jerold Jose* and M. Dev Anand**

ABSTRACT

Inconel 718 is the nickel based high strength super alloy suitable for service at temperature from (-252ºC) to (700ºC). It has been broadly used in components of gas turbines, nuclear plants and aircraft engines. Pulsed TIG welding is the main welding process adopted for welding of Inconel 718 alloy because of its welding quality and economy. Inconel 718 of 2mm thick plates was use as a base material. If the base material is 2mm with single pass weld, pulsed TIG welding is preferred over conventional TIG welding process. In this present research work, mechanical properties of Inconel 718 alloy is predict by developing empirical relationship. The pulsed TIG welding parameters such as Peak current, Base current, Pulse on time, Frequency and Shielding gas are consider as the input parameters. The experiments were conducted based on five-factor, three-level Box- Behnken design. Responds Surface Methodology (RSM) is one of the best the modeling tool use to develop the regression mathematical model to predict the mechanical properties of pulsed TIG welded Inconel 718 alloy. The developed models were checked for their suitability and consequence by ANOVA analysis. The developed mathematical model can be efficiently used to predict the mechanical properties of all the welded joints at the confidence level and it is acceptable one.

1. INTRODUCTION

Inconel 718 is a well known nickel based super alloy. It is extensively used for aerospace, power, and nuclear industries, because of its excellent mechanical properties and oxidation resistance at elevated temperature [1]. It has been proved that Inconel 718 has a good weldablity because of its resistance to weld solidification cracking [2-5]. According to the previous research some researchers reported that this alloy is more sensitive for segregation of alloying elements, formation of laves phases and micro-fissures at fusion zone or Heat Affected Zone (HAZ) [6]. Welding process like Electron Beam Welding (EBW), Laser Welding (LW) and TIG welding have been applied for joining of Inconel 718 alloy. However TIG welding process is widely used for joining of Inconel 718 alloy, because of its consistency of weld quality and overall economy.

Pulsed TIG (PTIG) welding is one of the variant of TIG welding process, in which the welding current is fed intermittently in the form of pulse. The pulsed current alternates between a low or base level and high or peak level. The duration and amplitude of both peak and base currents can be varied independently to suit the base metal to be welded .The melting take place during the peak current, and the weld pool solidifies between the pulses as the heat is dissipated in the base metal during the base current period. This current pulsing is to leads intermittent melting along the joint seam giving a series of discrete melt spots which overlap each other.

Wide range of investigation has been performed in this process and reported advantages include enhanced weld bead profile, superior tolerance to heat sink variations, lower heat input requirements minimize residual

* Research Scholar/Assistant Professor, Department of Mechanical Engineering, Noorul Islam Centre for Higher Education, Kumaracoil-629 180, Thuckalay, Kanyakumari District, Tamilnadu State, India, *Email: joseweld@gmail.com*

** Professor and Deputy Director Academic Affairs, Department of Mechanical Engineering, Noorul Islam Centre for Higher Education, Kumaracoil-629 180, Thuckalay, Kanyakumari District, Tamilnadu State, India, *Email: anandpmt@hotmail.com*

stresses and distortion [7]. Researchers frequently reported the metallurgical advantages of pulsed current welding, which include reûnement of fusion zone grain size and substructure, reduced width of HAZ and control of segregation [8], can lead to enhance the mechanical properties of the weld. Many researchers have been used current pulsing to achieve grain refinement in weld fusion zone for enhance the weld mechanical properties [9-10].

Different researchers have focused on the optimization of welding process parameters to achieve favorable mechanical properties, thus the mechanical properties of the welded joints are influenced by welding parameters of the respective welding process [11-15].There is a tendency in the direction of the application of statistical methods such as Design of Experiments (DOE), since experimental optimization of welding parameters is both time-consuming and expensive [16]. RSM is one of the most widely used method to describe the relationship between input parameters and output variable by develop the mathematical models.

There is number of research work have been carried out by researchers related to optimization of welding parameters of PTIG for achieving better mechanical properties for different materials [17-19]. However there is no data available regarding type of shielding gas is one of important welding input parameter for optimization. They have used RSM for optimization of PTIG cladding parameters for cladding of satellite alloy on carbon steel [20] and subsequently [21] have optimized welding parameters of friction welding process for dissimilar welded joint also [22] have reported for optimization of bead profile for submerged arc welded pipes by using RSM.

Although some researchers have already applied DOE to optimize welding parameters, but no effort is yet made to perform this optimization on PTIG welding of Inconel 718 alloy using RSM. This study is focused on the RSM optimization of some important welding parameters namely peak current, base current, pulse on time, frequency and shielding gas to achieve most favorable mechanical properties.

2. EXPERIMENTAL PLAN

2.1. Selection of Base Metal and Filler Wire

Super alloy Inconel 718 rolled sheets (2mm thick) in solution annealed (980ºC) are employed as a base material for this research work. The filler wire was an AWS classification ER NiFeCr-2 with 1.6mm diameter electrode. The chemical composition and mechanical properties of base metal are shown in Table 1 and 2 respectively.

2.2. Selection of Metal Joining Process

The PTIG welding process is choose as a metal joining process for this research work. This is based up on the suitability for the base metal and the specific advantages of PTIG welding process was reported by past research results [7-10].

Table 1
Chemical Composition of Base Metal

Element	*Ni*	*Cr*	*Nb*	*Mo*	*Ti*	*Al*	*C*	*B*	*Si*	*S*	*P*	*Fe*
wt. %	53	17.5	5.08	3.13	0.97	0.51	0.02	0.003	0.03	0.002	0.005	Bal

Table 2
Mechanical Properties of Base Metal

UTS (MPa)	*YS (MPa)*	*% Elongation*	*Hardness*
1034	829	20	40 HRC

2.3. Selection of Important Welding Parameters and Their Levels

The predominant welding parameters that independently control the mechanical properties of the welded joints are identified as peak current (P), base current (B), pulse on time (T), frequency (F) and shielding gas (S). Based on the several experimental trials the ranges of the parameters are decided. The three levels of welding parameters are listed in Table 3. The constant PTIG welding parameters are listed in Table 4.

2.4. Design of Experimentation (DOE) Based on RSM

RSM is a set of mathematical and statistical technique useful for modeling and analysis of problems. In this present study a Box-Behhen design with five factors and three levels was selected to conduct the experiment. Assume the numerical value of three levels of shielding gas is 1, 2, and 3 for helium (low level), argon (medium level), argon helium mixture (high level) respectively. The experimental design consists of 46 experiments that are shown in table 5.

Table 3
Welding Parameters and their Levels

Welding Parameter	*Notation*	*Level*		
		-1	*0*	*1*
Peak Current (A)	P	55	65	75
Base Current (A)	B	25	35	45
Pulse on Time (%)	T	40	50	60
Frequency (Hz)	F	2	4	6
Shielding Gas	S	Ar - 1	He - 2	Ar (70%)+He (30%) -3

Table 4
Constant Welding Parameters

Process Parameter	*Constant Value*
Argon (Ar) Flow Rate (l/min)	10
Helium (He) Flow Rate (l/min)	20
Ar (70%) + He (30%) Flow Rate (l/min)	15
Electrode Material	98% W + 2% Zr
Electrode Diameter, mm	2
Filler Wire	ER NiFeCr- 2
Filler Wire Diameter, mm	1.6

Table 5
Design of Experimentation (DOE)

Exp. No.	*Peak Current (Amp)*	*Base Current (Amp)*	*Pulse On Time (%)*	*Frequency (Hz)*	*Shielding Gas*
1	65	25	50	2	2
2	65	35	50	4	2
3	55	35	50	4	3
4	55	35	50	6	2
5	65	35	50	4	2
6	65	45	60	4	2

(contd...)

(Table 5 contd...)

Exp. No.	*Peak Current (Amp)*	*Base Current (Amp)*	*Pulse On Time (%)*	*Frequency (Hz)*	*Shielding Gas*
7	65	35	60	4	1
8	75	35	50	6	2
9	65	45	50	6	2
10	75	35	50	4	1
11	65	35	50	4	2
12	65	45	40	4	2
13	55	35	50	2	2
14	65	25	50	6	2
15	65	45	50	2	2
16	55	35	50	4	1
17	65	25	40	4	2
18	65	35	40	4	3
19	75	35	50	2	2
20	65	35	60	4	3
21	65	35	40	4	1
22	75	35	50	4	3
23	65	25	60	4	2
24	65	25	50	4	1
25	55	35	40	4	2
26	65	35	60	6	3
27	55	35	60	4	2
28	65	35	50	4	2
29	65	45	50	4	1
30	55	25	50	4	2
31	65	35	40	6	2
32	75	35	60	4	2
33	65	35	50	2	1
34	65	25	50	4	3
35	65	35	50	6	1
36	65	35	50	4	2
37	55	45	59	4	2
38	65	35	40	2	2
39	65	45	50	4	3
40	65	35	60	6	2
41	75	45	50	4	2
42	75	35	40	4	2
43	75	25	50	4	2
44	65	35	60	2	2
45	65	35	50	4	2
46	65	35	50	2	3

2.5. Conducting Experiment as per DOE

The base metal rolled sheets of dimension (150*60*2mm) was sliced by WEDM and they were grounded by surface grinder as shown in Fig. 1. Before welding base metal sheets were cleaned, wire burse and degreased by using acetone. The pair of base metal sheets were kept together to form a tight square butt configuration by using mechanical clamp and fixtures as shown in Fig. 2. An automatic TIG welding machine with pulsed mode has been used for preparation of square but joint welded test coupon. Forty-six pairs of base metals were welded based on the welding parameters assigned by DOE shown in table 5.Photgraph of welded test coupons are displayed in Fig. 3.

2.6. Preparation of Test Specimens

Tensile test specimens were taken at the middle of the test coupon. They were machined according to ASTM E8 standards (23). The configuration tensile test specimen used for machining is shown in Fig. 4. Three samples for each welded test coupon were machined to ensure repeatability of the tensile strength. Photograph of the tensile specimens are shown in Fig. 5. The specimens for micro hardness tests were located at the middle of the welded test coupon

2.7. Post Weld Aging Heat Treatment

Test specimens of both tensile and micro hardness were aged according to ASTM B637. It consisted of heating at 718ºC for 8 hours and furnace cooled (at 55ºc/hour) to 621ºC and maintain 621ºC for 18 hours and air cooled to room temperature.

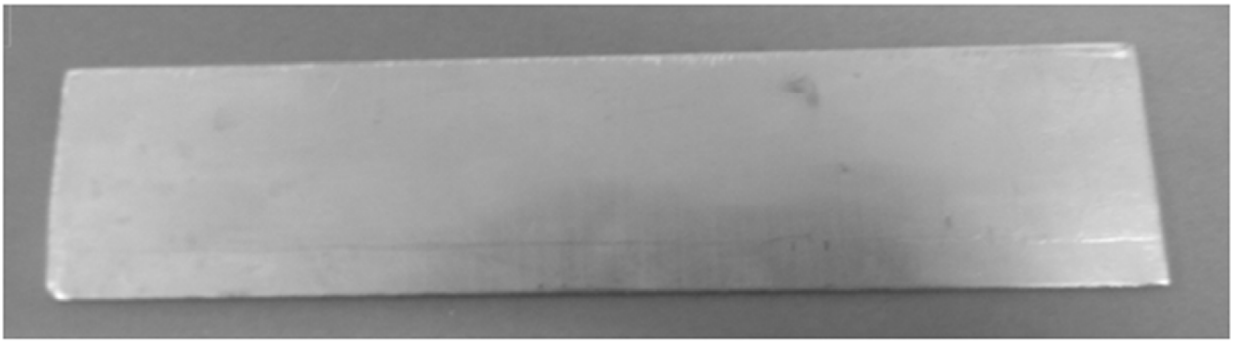

Figure 1: Base Metal

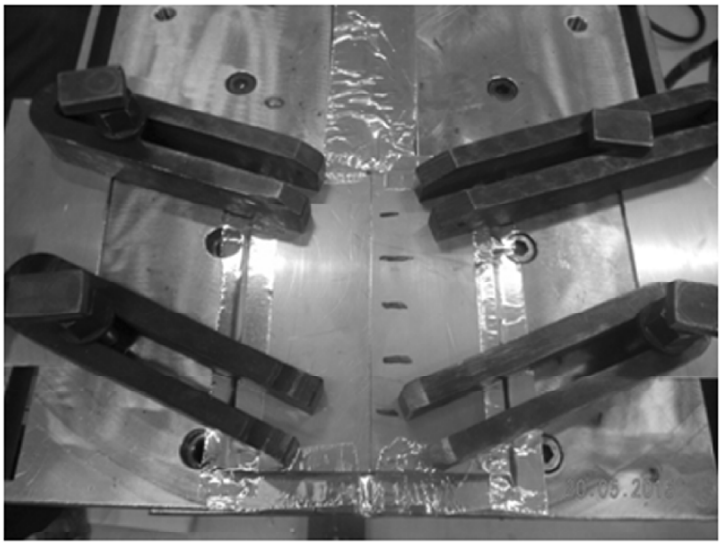

Figure 2: Photography of Square Butt Weld Joint Preparation

2.8. Measurement of Mechanical Properties (Responds)

Tensile test specimens were tested using a computer controlled Instron 3369 tensile tester machine. Micro hardness specimens were polished by disc polisher with different grit (200-1200) SiC emery paper and etched by standard regent glyceregia. A digital Vickers hardness tester was used to measure the hardness. The Vickers hardness load was 2.942N and duration of 15 sec.

The mechanical properties, i.e. Ultimate Tensile Strength (UTS), Yield Strength (YS), Percentage Elongation (%E) and Micro Hardness (H) of the welded test coupon were evaluated and present in the Table 6.

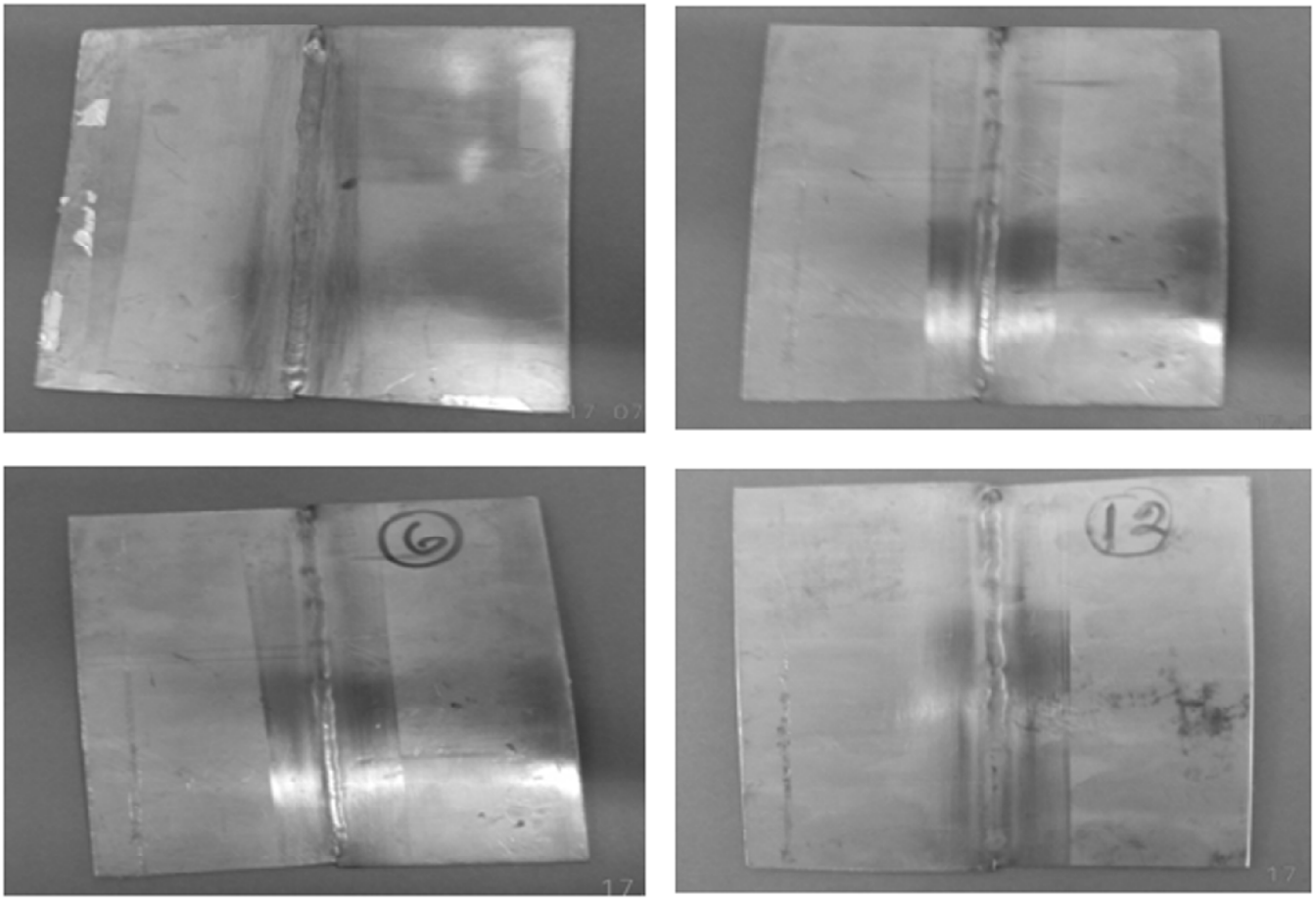

Figure 3: Welded Test Coupon

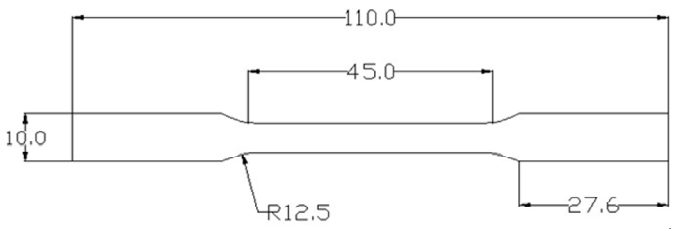

Figure 4: Configuration of Tensile Specimen

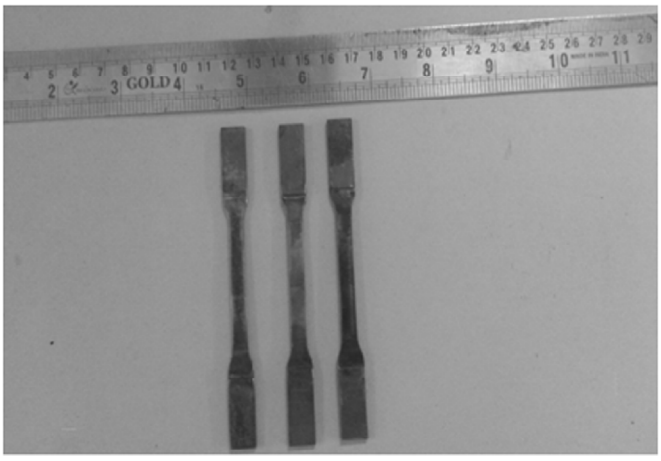

Figure 5: Tensile Test Specimen

Table 6
Experimental Results–Mechanical Properties

Exp. No.	*UTS (MPa)*	*YS (MPa)*	*% Elongation*	*Hardness (VHN)*
1	1340	1110	6.7	406
2	1282	1065	5.8	388
3	1372	1137	7.1	415
4	1389	1142	7.2	415
5	1279	1061	5.7	387
6	1253	1040	5.2	375
7	1250	1043	5.6	378
8	1285	1070	5.9	388
9	1252	1039	5.3	377
10	1230	1030	5.4	371
11	1276	1063	5.7	386
12	1252	1046	5.3	376
13	1361	1131	7.2	412
14	1374	1142	7.3	416
15	1240	1038	5.1	372
16	1355	1125	7	409
17	1390	1153	7.3	422
18	1306	1085	6	396
19	1238	1036	5.2	371
20	1269	1053	5.6	382
21	1295	1076	5.9	392
22	1246	1049	5.3	374
23	1285	1061	5.7	388
24	1337	1112	7	403
25	1386	1150	7.4	420
26	1288	1072	5.8	391
27	1310	1087	6.1	396
28	1275	1060	5.7	386
29	1232	1029	5	372
30	1427	1181	7.9	433
31	1325	1101	6.8	401
32	1234	1031	5.2	373
33	1288	1069	6	390
34	1368	1135	6.9	413
35	1273	1056	5.8	385
36	1279	1061	5.8	387
37	1269	1054	5.6	384
38	1291	1073	5.9	391
39	1246	1049	5.2	372
40	1280	1063	5.7	387
41	1230	1027	5.1	370
42	1261	1051	5.4	381
43	1271	1060	5.7	385
44	1244	1043	5.3	374
45	1276	1063	5.7	386
46	1271	1056	5.6	382

2.9. Development of Performance Model

A procedure based on regression was used for development of mathematical models and to predict the mechanical properties [23].

In this research, the response function (Y) is the functions of welded joint, i.e. UTS, YS, E and H. They are the functions of peak current (P), Base current (B), Pulse on time (T), Frequency (F) and shielding gas (S).

$$Y = f(P, B, T, F, S)$$

The second order polynomial (regression) equation that represents the response function 'Y'

$$Y = b_{0+} \sum b_i x_i + \sum b_{ii} x_i^2 + \sum b_{ij} x_i x_j$$

Where b_0 denote for average response and b_i, b_{ij} is meant for the coefficient that represent for main and interactive effect of parameters. Consider five parameters, the selected predicted equation could be expressed as;

$$Y = b_0 + b_1 (P) + b_{-2} (B) + b_3 (T) + b_4 (F) + b_5 (S) + b_{11} (P^2) + b_{22} (B^2) + b_{33} (T^2) + b_{44} (F^2) + b_{55} (S^2) + b_{12}(PB) + b_{13} (PT) + b_{14} (PF) + b_{15}(PS) + b_{23}(BT) + b_{24} (BF) + b_{25} (BS) + b_{34} (TF) + b_{35} (TS) + b_{45}(FS)$$

In this present research work, Box- Behnken design which accurately fit the second order responds surface was used. All the coefficients were obtained by applying Box- Behnken design using the minitab-14 software package. The final mathematical model to predict tensile strength and hardness of PTIG welded Inconel 718 alloy was obtained as;

UTS=4376.85+(P*-48.4387)+(B*-40.4682)+(T*-17.5359)+(F*-30.3245)+(S*-7.79475)+(P*P*0.200274)+(B*B*0.118607)+(T*T*0.0204913)+(F*F*2.73485)+(S*S*1.52274)+(P*B* 0.256688)+(P*T*0.13934)+(P*F*0.2375)+(P*S*-0.025)+(B*T*0.24816)+(B*F*-0.275)+(B*S* -0.425)+(T*F* -0.119138)+(T*S* -0.0882766)+(F*S* 7.78361)

YS = 3656.95+(P* -41.6218)+(B* -32.6)+(T* -14.1917)+(F* -22.2349)+(S* -34.6157)+(P*P* 0.174783)+(B*B*0.10395)+(T*T*-0.0175087)+(F*F*2.17529)+(S*S*3.28451) (P*B*0.202672)+(P*T* 0.122887)+(P*F* 0.2875)+(P*S* 0.175)+(B*T*0.199613)+(B*F* -0.3875)+(B*S* -0.075)+(T*F* -0.190997)+(T*S* -0.156993)+(F*S* 7.07568)

%E=55.1997+(P*-0.814427)+(B*-0.591509)+(T*-0.257227)+(F*-0.582994)+(S*-0.470156) +(P*P*0.003442)+(B*B*0.001442)+(T*T*-0.000475278)+(F*F*0.0535355)+(S*S*0.0808088) +(P*B*0.00356286)+(P*T*0.00277348)+(P*F*0.00875)+(P*S*-0.005)+(B*T*0.00372652) +(B*F*-0.005)+(B*S* 0.0075)+(T*F* -0.00771776)+(T*S* -0.00543553)+(F*S* 0.126771)

H=1334+(A2*-14.2545)+(B2*-11.8466)+(C2*-5.91311)+(D2*-18.7075)+(E2*7.02243) +(A2*A2*0.0560782)+(B2*B2*0.0285782)+(C2*C2*-0.00353812)+(D2*D2*0.689055) +(E2*E2*0.00621973)+(A2*B2* 0.0751673)+(A2*C2* 0.0413024)+(A2*D2* 0.175)+(A2*E2* -0.075)+(B2*C2*0.0811976)+(B2*D2*-0.0625)+(B2*E2*-0.25)+(C2*D2* 0.010779)+(C2*E2* -0.0534421)+(D2*E2* 2.83923)

The above equations are represents the individual and interactive effects of PTIG welding parameters on mechanical properties of Inconel 718 alloy.

2.10. Check the Satisfactoriness of the Prediction Model

The Analysis Of Variance (ANOVA) technique was used to check the developed models. The results of ANOVA for UTS, YS % E & H are representing the table. The results show that the predication model is

Table 7
Analysis of Variance for UTS (MPa)

Source	*DF*	*F*	*Adj SS*	*Adj MS*	*Seq SS*	*P*
Regression	20	60.83	115301	115301	5765/0	0.000
Linear	5	217.95	103132	103279	20655.7	0.000
Square	5	10.71	5543	5076	1015.2	0.000
Interaction	10	6.99	6626	6626	662.6	0.000
Residual Error	25		2369	2369	94.8	
Lack-of-Fit	20	16.75	2334	2334	116.7	0.003
Pure Error	5		35	35		
Total	45		117670			

Table 8
Analysis of Variance for YS (Mpa)

Source	*DF*	*Seq SS*	*Adj SS*	*Adj MS*	*F*	*P*
Regression	20	69005.2	69005.2	3450.3	61.80	0.000
Linear	5	60320.8	60507.2	12101.4	216.75	0.000
Square	5	3966.3	3662.3	732.5	13.12	0.000
Interaction	10	4718.1	4718.1	471.8	8.45	0.000
Residual Error	25	1395.8	1395.8	55.8		
Lack-of-Fit	20	1378.9	1378.9	68.9	20.48	0.002
Pure Error	5	16.8	16.8	3.4		
Total	45	70401.0				

Table 9
Analysis of Variance for Elongation (%)

Source	*DF*	*Seq SS*	*Adj SS*	*Adj MS*	*F*	*P*
Regression	20	25.5759	25.5759	1.27879	44.62	0.000
Linear	5	22.2694	22.2857	4.45715	155.52	0.000
Square	5	1.5095	1.4441	0.28881	10.08	0.000
Interaction	10	1.7970	1.7970	0.17970	6.27	0.000
Residual Error	25	0.7165	0.7165	0.02866		
Lack-of-Fit	20	0.7032	0.7032	0.03516	13.18	0.005
Pure Error	5	0.0133	0.0133	0.00267		
Total	45	26.2924				

Table 10
Analysis of Variance for Hardness (VHN)

Source	*DF*	*Seq SS*	*Adj SS*	*Adj MS*	*F*	*P*
Regression	20	11564.3	11564.3	578.21	105.75	0.000
Linear	5	10426.7	10458.3	2091.66	382.55	0.000
Square	5	415.0	373.6	74.72	13.67	0.000
Interaction	10	722.7	722.7	72.27	13.22	0.000
Residual Error	25	136.7	136.7	5.47		
Lack-of-Fit	20	133.4	133.4	6.67	10.00	0.009
Pure Error	5	3.3	3.3	0.67		
Total	45	11701.0				

significant with linear and quadratic terms for all four models. All the four models have P value is less than .05. It is understood that the developed predication model is valid at 95% confidence level.

2.11. Validation of Predication Model

Validation of predication model where carried out by calculation of percentage error by using below relation.

$$\% \ Error = \frac{Experimental \ value - predicted \ value}{predicted \ value} * 100$$

The result of error calculation for all response functions are presents in Table 11 and 12. It is found that all the four predicated models where able to predict UTS, YS, % E and H with acceptable accuracy.

3. RESULTS AND DISCUSSION

The effect of five process parameters i.e. peak current, base current, pulse on time, frequency, and shielding gas and their effects on UTS, YS, %E and H is analyzed and studied using the experimental value. Experimental values are plotted as a counter plot and they are displayed in Figs. (6-10). The plotted counter plots are efficiently used to understand the effect of PTIG welding parameters on mechanical properties of PTIG welded Inconel 718 alloy joint.

3.1. Effect Welding Parameters on UTS

Fig. 6 displays the effect of welding parameters on UTS. Fig. 6a shows that maximum UTS value is obtained at the peak current of 55 Amp (low level) and at the base current of 25Amp (low level). It is understood that UTS value is inversely proportional to peak current and base current value. From Fig. 6b it is clear that maximum value of UTS can be obtained at the pulse on time of 40 % (low level). Fig. 6c, 6d shows that maximum value of UTS is can be achieved at the frequency of 6Hz (high level) and the shielding gas of argon and argon helium mixture.

3.2. Effect Welding Parameters on YS

Fig. 7 displays the effect of welding parameters on YS. Fig. 7a shows that maximum YS value is obtained at the peak current of 55 Amp (low level) and at the base current of 25Amp (low level). It is understood that YS value is inversely proportional to peak current and base current value. From Fig. 7b it is clear that

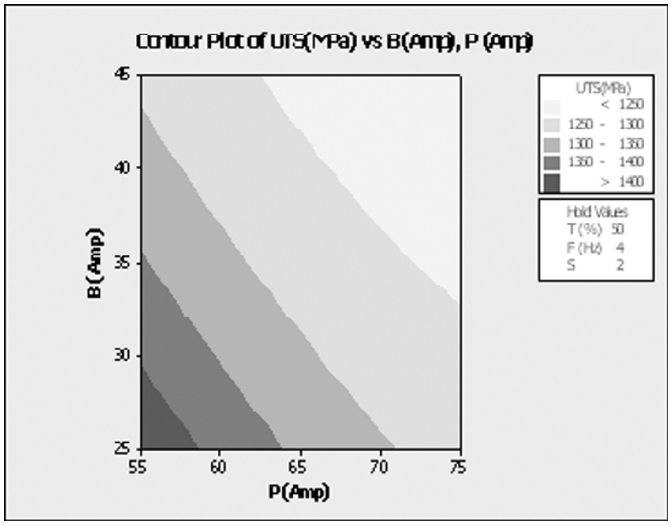

(a) Peak Current Vs Base current

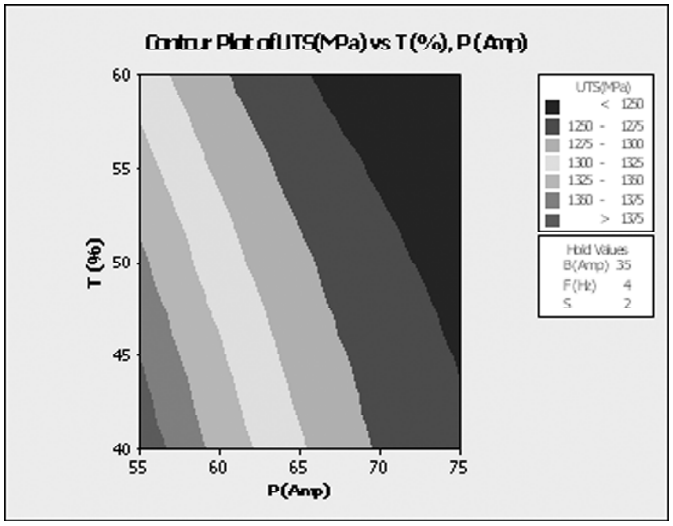

(b) Peak Current Vs Pulse On Time

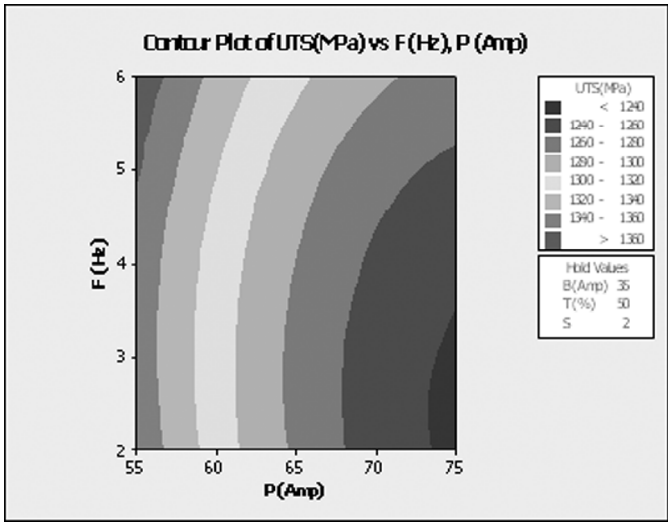

(c) Peak Current Vs Frequency

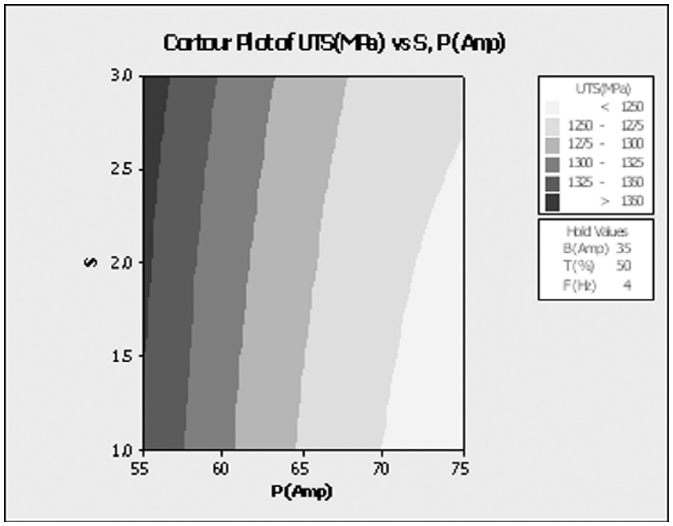

(d) Peak Current Vs Shielding Gas

Figure 6: Effect of Welding Parameters on UTS

Table 11
Measurement of Error for UTS & YS

Exp. No.	*UTS (MPa) Experimental Value*	*UTS (MPa) Predicted Value*	*% Error*	*Max. Error*	*YS (MPa) Experimental Value*	*YS (MPa) Predicted Value*	*% Error*	*Max. Error*
1	1340	1332.876	0.534475		1110	1103.486	0.590321	
2	1282	1279.300	0.211025		1065	1063.236	0.165918	
3	1372	1365.137	0.502710		1137	1131.596	0.477599	
4	1389	1374.991	1.018814		1142	1135.075	0.610126	
5	1279	1279.300	0.023478		1061	1063.236	0.210292	
6	1253	1238.744	1.150870		1040	1032.685	0.70832	
7	1250	1246.186	0.306089		1043	1038.150	0.467205	
8	1285	1273.451	0.906874		1070	1063.332	0.627103	
9	1252	1260.325	0.660528		1039	1045.678	0.638649	
10	1230	1237.064	0.571003		1030	1032.902	0.280946	
11	1276	1279.300	0.257981		1063	1063.236	0.022187	
12	1252	1239.020	1.047571		1046	1033.691	1.190746	
13	1361	1356.583	0.325604		1131	1126.999	0.355023	
14	1374	1371.785	0.161498		1142	1138.562	0.301994	
15	1240	1243.416	0.274752		1038	1041.602	0.345861	
16	1355	1347.604	0.548850		1125	1119.645	0.478304	
17	1390	1389.112	0.063913		1153	1150.997	0.173991	
18	1306	1313.128	0.542819		1085	1094.529	0.870622	
19	1238	1236.043	0.158335		1036	1032.256	0.362691	
20	1269	1261.454	0.598225		1053	1050.461	0.241734	
21	1295	1294.329	0.051862		1076	1075.939	0.005713	
22	1246	1253.597	0.606041	1.15087	1049	1051.853	0.271209	1.190746
23	1285	1289.571	0.354496		1061	1070.146	0.854658	
24	1337	1330.147	0.515216		1112	1107.132	0.439722	

(contd...)

(Table 11 contd...)

Exp. No.	*UTS (MPa) Experimental Value*	*UTS (MPa) Predicted Value*	*% Error*	*Max. Error*	*YS (MPa) Experimental Value*	*YS (MPa) Predicted Value*	*% Error*	*Max. Error*
25	1386	1391.687	0.408639		1150	1153.338	0.2894	
26	1288	1299.532	0.887379		1072	1079.281	0.674626	
27	1310	1313.910	0.297606		1087	1087.832	0.076453	
28	1275	1279.300	0.336149		1060	1063.236	0.304344	
29	1232	1238.187	0.499688		1029	1031.248	0.218017	
30	1427	1442.607	1.081871		1181	1191.689	0.897003	
31	1325	1329.482	0.337122		1101	1104.258	0.295069	
32	1234	1230.738	0.265022		1031	1029.166	0.178175	
33	1288	1284.859	0.244490		1069	1071.86	0.266794	
34	1368	1355.681	0.908731		1135	1124.083	0.971235	
35	1273	1281.633	0.673570		1056	1063.133	0.670909	
36	1279	1279.300	0.023478		1061	1063.236	0.210292	
37	1269	1276.485	0.586364		1054	1060.841	0.644859	
38	1291	1296.808	0.447867		1073	1077.043	0.375354	
39	1246	1246.721	0.057809		1049	1045.199	0.363652	
40	1280	1274.808	0.407296		1063	1055.690	0.692461	
41	1230	1231.107	0.089948		1027	1031.063	0.394088	
42	1261	1252.779	0.656223		1051	1045.518	0.524375	
43	1271	1280.230	0.720930		1060	1067.912	0.740912	
44	1244	1251.665	0.612368		1043	1043.754	0.072232	
45	1276	1279.300	0.257981		1063	1063.236	0.022187	
46	1271	1270.758	0.019055		1056	1059.008	0.284016	

Table 12
Measurement of Error for %E & H

Exp. No.	% Elongation Experimental Value	% Elongation Predicted Value	% Error	Max. Error	Hardness (VHN) Experimental Value	Hardness (VHN) Predicted Value	% Error	Max. Error
1	1340	6.565315	2.051468		1110	403.3367	0.660316	
2	1282	5.743790	0.978627		1065	386.8886	0.287254	
3	1372	7.030614	0.986910		1137	412.5434	0.595478	
4	1389	7.126449	1.032089		1142	413.3560	0.397727	
5	1279	5.743790	0.762383		1061	386.8886	0.028782	
6	1253	5.078618	2.390062		1040	372.9675	0.544949	
7	1250	5.447614	2.797292		1043	376.9272	0.284625	
8	1285	5.904591	0.077748		1070	385.9888	0.521051	
9	1252	5.438949	2.554698		1039	379.1687	0.571954	
10	1230	5.406983	0.129144		1030	373.9620	0.792053	
11	1276	5.743790	0.762383		1063	386.8886	0.22969	

(contd...)

(Table 12 contd...)

Exp. No.	% Elongation Experimental Value	% Elongation Predicted Value	% Error	Max. Error	Hardness (VHN) Experimental Value	Hardness (VHN) Predicted Value	% Error	Max. Error
12	1252	5.049164	4.967874		1046	372.8104	0.855566	
13	1361	7.049673	2.132401		1131	411.5166	0.117475	
14	1374	7.192091	1.500388		1142	414.6761	0.319261	
15	1240	5.212173	2.152129		1038	372.8293	0.222427	
16	1355	6.878841	1.761332		1125	406.8291	0.533603	
17	1390	7.347610	0.647964		1153	422.0573	0.013579	
18	1306	6.215238	3.463065		1085	397.2238	0.308084	
19	1238	5.127815	1.407721		1036	370.1494	0.229799	
20	1269	5.390677	3.883054	4.967874	1053	380.0726	0.507120	0.855566
21	1295	6.054754	2.555904		1076	391.9407	0.015132	
22	1246	5.358756	1.096452		1049	376.6762	0.710484	
23	1285	5.886456	3.167541		1061	389.7354	0.445283	
24	1337	6.794483	3.024766		1112	401.6493	0.336294	
25	1386	7.461664	0.826410		1150	421.4977	0.355319	
26	1288	5.917394	1.983878		1072	393.1425	0.544977	
27	1310	6.191118	1.471752		1087	397.1548	0.290773	
28	1275	5.743790	0.762383		1060	386.8886	0.229690	
29	1232	5.091341	1.794042		1029	373.6418	0.439417	
30	1427	8.150976	3.079088		1181	436.5583	0.815084	
31	1325	6.636072	2.470255		1101	401.5364	0.133576	
32	1234	5.173956	0.503369		1031	371.0481	0.526043	
33	1288	6.053008	0.875727		1069	388.8027	0.307940	
34	1368	6.696256	3.042652		1135	410.8635	0.519996	
35	1273	5.972700	2.891486		1056	386.2852	0.332708	
36	1279	5.743790	0.978627		1061	386.8886	0.028782	
37	1269	5.610405	0.185464		1054	384.5843	0.151941	
38	1291	5.900586	0.009926		1073	393.1281	0.541329	
39	1246	5.293114	1.759157		1049	372.8561	0.229605	
40	1280	5.611512	1.576907		1063	385.8852	0.288907	
41	1230	5.025976	1.472834		1027	369.1837	0.221105	
42	1261	5.335110	1.216284		1051	378.8700	0.562195	
43	1271	5.866546	2.838906		1060	387.1577	0.557315	
44	1244	5.493446	3.521398		1043	376.6146	0.694236	
45	1276	5.743790	0.762383		1063	386.8886	0.229690	
46	1271	5.597697	0.041138		1056	381.6601	0.089071	

maximum value of YS can be obtained at the pulse on time of 40 % (low level). Fig. 7c, 7d shows that maximum value of YS is can be achieved at the frequency of 6Hz (high level) and the shielding gas of argon and argon helium mixture.

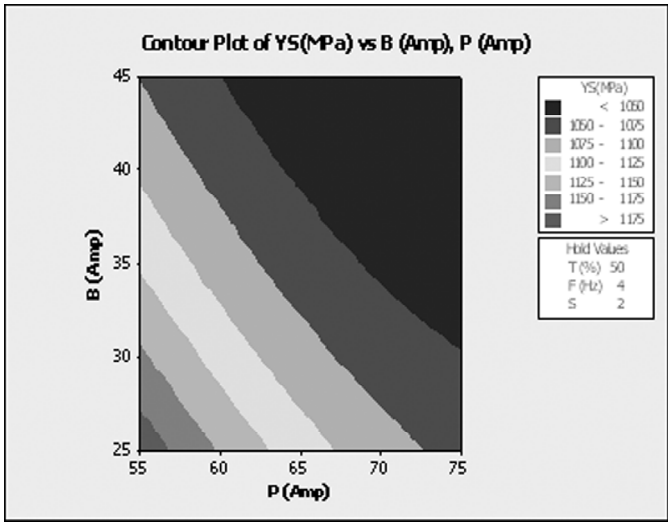

(a) Peak Current Vs Base Current

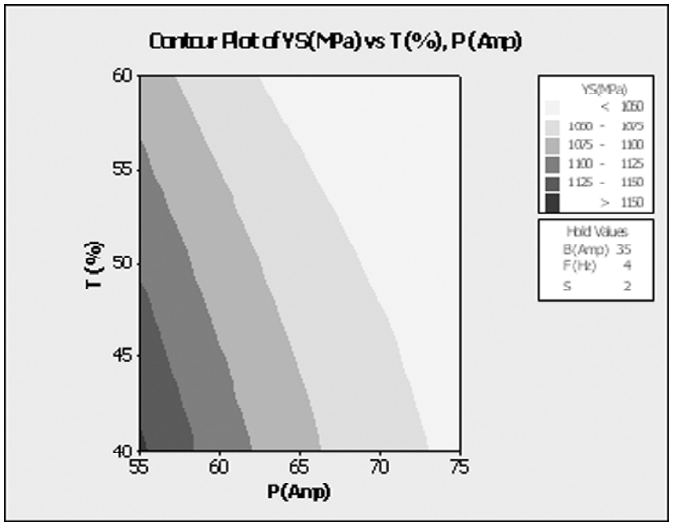

(b) Peak Current Vs Pulse On Time

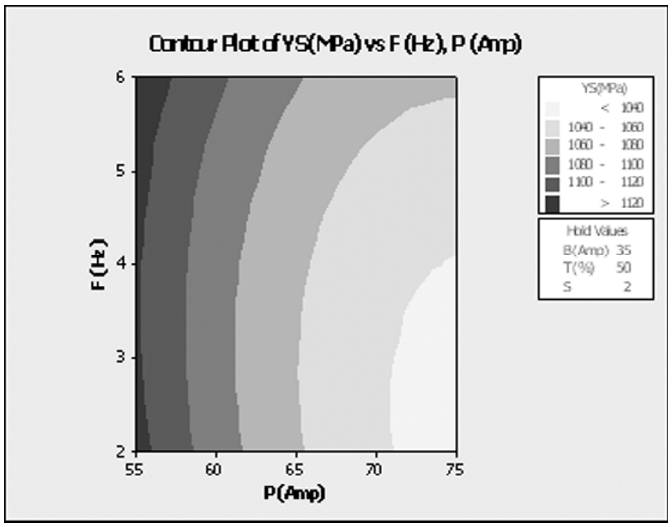

(c) Peak current Vs Frequency

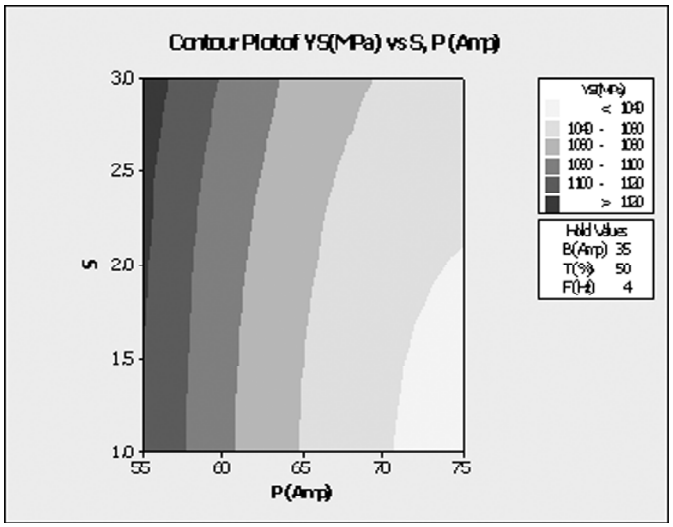

(d) Peak Current Vs Shielding Gas

Figure 7: Effect of Welding Parameters on YS

3.3. Effect Welding Parameters on %E

Fig. 8 displays the effect of welding parameters on percentage elongation. Fig. 8a shows that maximum UTS value is obtained at the peak current of 55 Amp (low level) and at the base current of 25Amp (low level). It is understood that elongation value is inversely proportional to peak current and base current value. From Fig. 8b it is clear that maximum value of elongation can be obtained at the pulse on time of 40 % (low level). Fig. 8c, shows that maximum value of elongation is can be achieved at the frequency of 6Hz (high level) .Fig 8d revels that type of shielding gas not makes much impact on elongation.

3.4. Effect Welding Parameters on Hardness

Fig. 9 displays the effect of welding parameters on Hardness. Fig. 9a shows that maximum hardness value is obtained at the peak current of 55 Amp (low level) and at the base current of 25Amp (low level). It is means that hardness value is inversely proportional to peak current and base current value. From Fig. 9b it is clear that maximum value of hardness can be obtained at the pulse on time of 40 % (low level). Fig. 9c, 9d shows that maximum value of hardness can be achieved at the frequency of 6Hz (high level) and the shielding gas of argon and argon helium mixture.

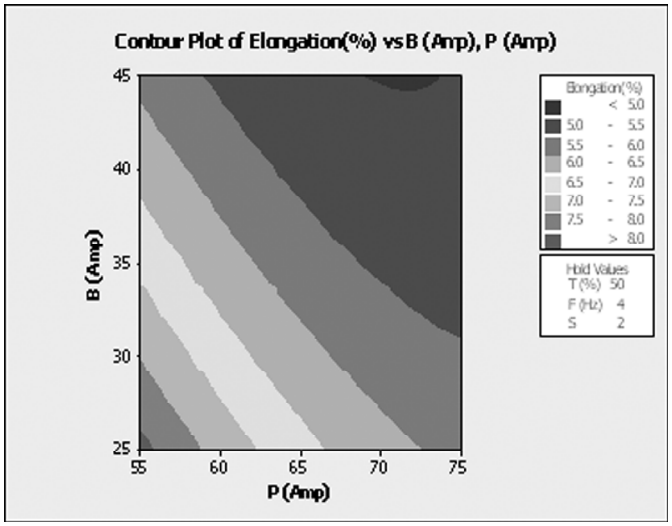

(a) Peak Current Vs Base Current

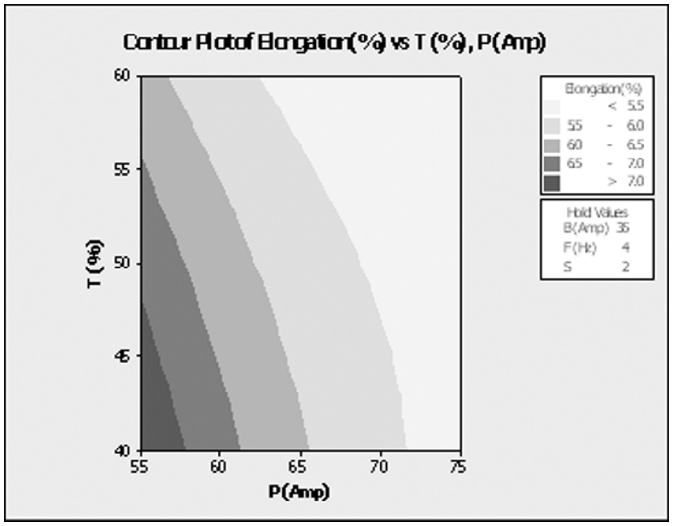

(b) Peak Current Vs Pulse On Time

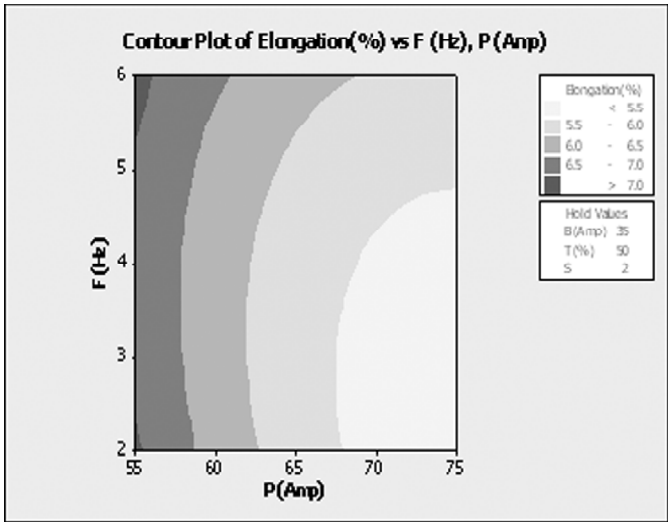

(c) Peak Current Vs Frequency

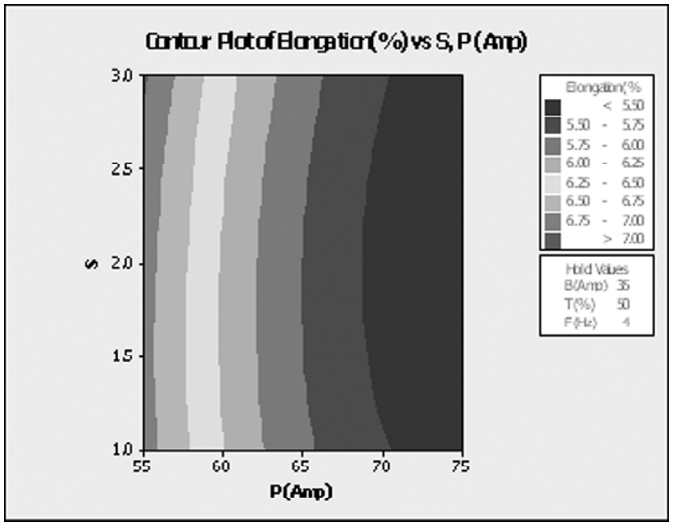

(d) Peak Current Vs Shielding Gas

Figure 8: Effect of Welding Parameters on %E

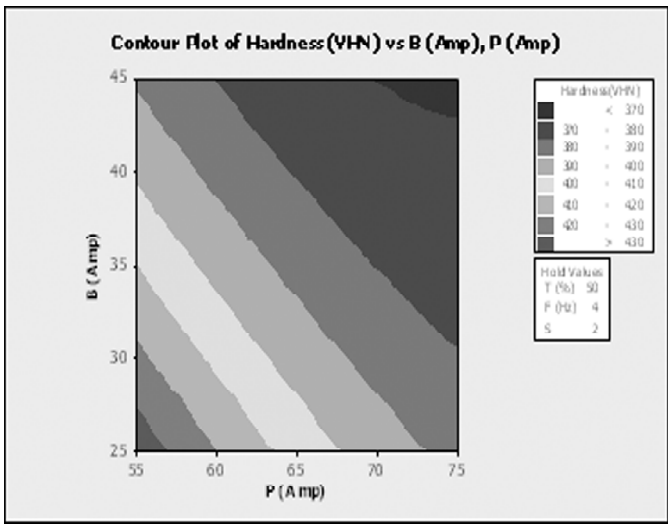

(a) Peak Current Vs Base Current

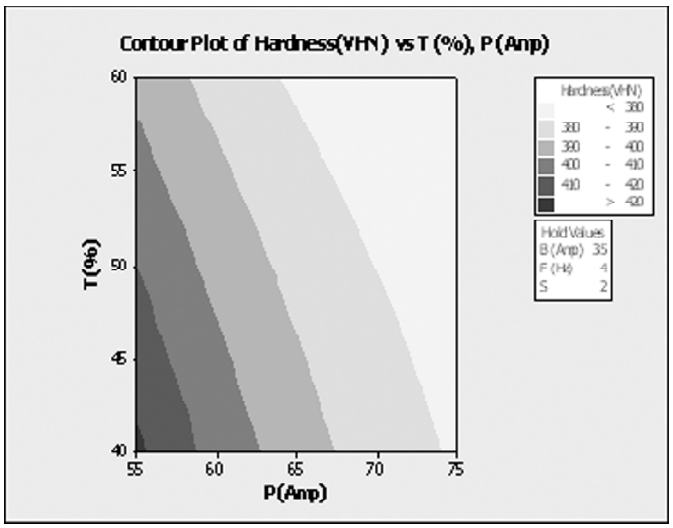

(b) Peak Current Vs Pulse On Time

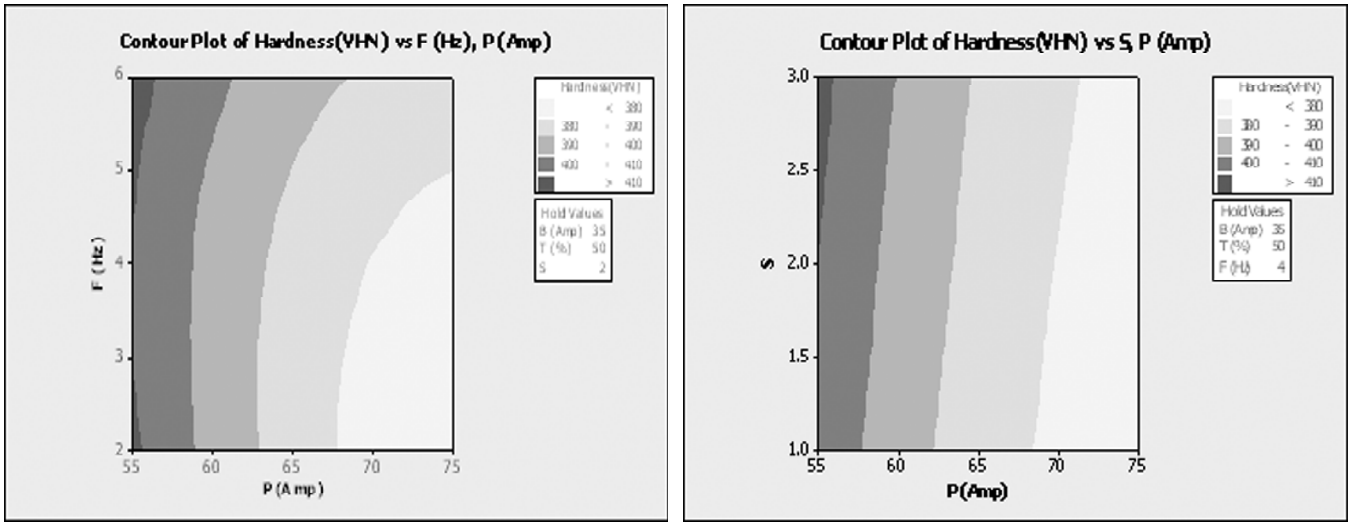

(c) Peak Current Vs Frequency **(d) Peak Current Vs Shielding Gas**

Figure 9: Effect of Welding Parameters on Hardness

4. CONCLUSION

Based on the result obtained from the experiments conducted to study the mechanical properties of Inconel 718 alloy using PTIG welding the following findings were made, The effect of PTIG welding parameters like peak current, base current, pulse on time, frequency, and shielding gas on UTS,YS, percent elongation and hardness in welding of Inconel 718 alloy has been studied. Experiments were conducted using Box-Behknen method and mathematical models have been developed. From the study it was observed that the peak current has the most significant effect on UTS, YS, percent Elongation and hardness and followed by base current, frequency, shielding gas and pulse on time. However pulse on time has least significant influence on UTS, Yield strength, percent Elongation and Hardness. Optimum mechanical properties like UTS,YS, percentage elongation and hardness was obtained by when peak current is 65Amp, base current is25 Amp, pulse on time is 40%, frequency is 4Hz and the shielding gas is argon.

REFERENCES

[1] Hsuan–Liang Lin, Tong–Min Wu. Effect of activating flux on weld bead geometry of Inconel 718 alloy of TIG welds, Journal of Materials and Manufacturing Process, Vol. 27 2012, 1457-61

[2] A. Lingenfelter, Welding of Inconel 718–a Historical Review, in: E.A. Loria (Ed.), Conference Proceedings on Superalloy 718–Metallurgy and Applications, TMS-AIME, Warrendale, PA, 1989, p. 673.

[3] R.G. Thompson, Micro-ûssuring of Inconel 718 in the Weld HAZ, Journal of Materials, Vol. 40 (7), 1988, 44.

[4] G. Cam, M. Kocak, Progress in Joining of Advanced Materials, International Material Review, Vol. 43 (1),1998, 1

[5] N.L. Richards, M.C. Chaturvedi, Effect of Minor Elements on Weldability of Nickel Base Superalloys, International Material Review, Vol. 45,2000, 109

[6] J.K. Hong, J.H. Park. Micro Structure and Mechanical Properties of Inconel 718 Welds by CO_2 Laser Welding. Journal of Materials Processing Technology, Vol. 201, 2008, 515-520

[7] Ravi Vishnu P. Welding World, Vol. 35(4), 1995, 214–20.

[8] Gokhale A.A, Tzavaras D.J, Brody H.D, Ecer G.M. International Proceedings of Conference on Grain Reûnement in Casting and Welds. St. Louis (MO): TMS-AIME; 1982, 223–47.

[9] Madhusudhan Reddy G, Gokhale A A., Journal of Material Science, Vol. 32(1993), 1997; 4117–41126.

[10] Yamamoto H. Weld International, Vol. 7(6),1993, 456–462.

[11] Gharibshahiyan E, Honarbakhsh Raou A, Parvin N, Rahimian M, The Effect of Microstructure on Hardness and Toughness of Low Carbon Welded Steel Using Inert Gas Welding, Material and Design, Vol. 32, 2011; 2042–2048.

[12] Honarbakhsh-Raouf A, Ghazvinloo H R. Inûuence of Wire Feeding Speed, Welding Speed and Preheating Temperature on Hardness and Microstructure of Weld of RQT 701-British Steel Produced by FCAW, Indian Journal of Science and Technology, Vol. 5, 2010, 588–591.

[13] Karadeniz E, Ozsarac U, Yildiz C. The Effect of Process parameters on Penetration in Gas Metal Arc Welding Processes, Material and Design, Vol. 28, 2007, 649–656.

[14] Acherjee B, Misra D, Bose D, Venkadeshwaran K., Prediction of Weld Strength and Seam Width for Laser Transmission Welding of Thermoplastic Using Response Surface Methodology. Optical Laser Technology, Vol. 41, 2009, 956–967.

[15] Vasudevan M, Kuppuswamy M V, Bhaduri A K., Optimizing Process Parameters for Gas Tungsten Arc Welding of an Austenitic Stainless Steel Using Genetic Algorithm, Trans Indian Intuitions of Metals, Vol. 63(1), 2010, 1–10.

[16] N. Kiaee, M. Aghaie – Khafri., Optimization of Gas Tungsten Arc Welding Process by Response Surface Methodology, Journal Material and Design, Vol. 54, 2014, 25-31.

[17] M. Balasubramanian, V. Jayabalan, V. Balasubramanian., Effect of Pulsed Gas Tungsten Arc Welding on Corrosion Behavior of Ti–6Al–4V Titanium Alloy. Journal of Material and Design, Vol. 29, 2008, 1359-63.

[18] T. Senthil Kumar, V. Balasubramanian, M.Y. Sanavullah, Influences of Pulsed Current Tungsten Inert Gas Welding Parameters on the Tensile Properties of AA6061 Aluminium Alloy, Journal of Material and Design, Vol. 28, 2007, 2080-2092.

[19] A. Razal Rose, K. Manisekar, V. Balasubramanian., Prediction and Optimization of Pulsed Current Tungsten Inert Gas Welding Parameters to Attain Maximum Tensile Strength in AZ61A Magnesium Alloy, Journal of Material and Design, Vol. 37, 2012, 334-348.

[20] F. Madadi, F. Ashrafizaden, M. Shamanian., Optimization of Pulsed TIG Cladding Process of Satellite Alloy on Carbon Steel Using RSM, Journal of Alloy and Compounds, Vol. 501, 2012, 71-78.

[21] Paventhan R, Lakshminarayanan P R, Balasubramanian V., Optimization of Friction Welding Process Parameters for Joining Carbon Steel and Stainless Steel, Journal of Iron and Steel Research Institute, Vol. 19, 2012, 66–71.

[22] T.B. Barker, Quality by Experiment and Design, ASQC Quality Press: Marcel Dekker: 1985.

[23] N. Ganaraj, N. Murugan., Prediction and Control of Weld Bead Geometry and Shape Relationships in Submerged Arc Welding of Pipes, Journal of Material Processing Technology, Vol. 168, 2005, 478–487.